Article

An Underestimated Contribution of Deltaic Denitrification in Reducing Nitrate Export to the Coastal Zone (Po River–Adriatic Sea, Northern Italy)

Maria Pia Gervasio [ID], Elisa Soana *[ID], Fabio Vincenzi and Giuseppe Castaldelli [ID]

DiSAP—Department of Environmental and Prevention Sciences, University of Ferrara, Via L.Borsari 46, 44121 Ferrara, Italy; grvmrp@unife.it (M.P.G.); fabio.vincenzi@unife.it (F.V.); ctg@unife.it (G.C.)
* Correspondence: elisa.soana@unife.it

Abstract: In transitional environments, the role of sediments biogeochemistry and denitrification is crucial for establishing their buffer potential against nitrate (NO_3^-) pollution. The Po River (Northern Italy) is a worldwide hotspot of eutrophication. However, benthic N dynamics and the relevance of denitrification in its delta have not yet been described. The aim of the present study was to quantify the contribution of denitrification in attenuating the NO_3^- loading transported to the sea during summer. Benthic fluxes of dissolved inorganic nitrogen (N) and denitrification rates were measured in laboratory incubations of intact sediment cores collected, along a salinity gradient, at three sections of the Po di Goro, the southernmost arm of the Po Delta. The correlation between NO_3^- consumption and N_2 production rates demonstrated that denitrification was the main process responsible for reactive N removal. Denitrification was stimulated by both NO_3^- availability in the Po River water and organic enrichment of sediment likely determined by salinity-induced flocculation of particulate organic load, and inhibited by increasing salinity, along the river–sea gradient. Overall, denitrification represented a sink of approximately 30% of the daily N loading transported in middle summer, highlighting a previously underestimated role of the Po River Delta.

Keywords: denitrification; Po River; nitrate loading; eutrophication; river sediment

1. Introduction

Rivers draining agricultural and urban basins export high quantities of reactive nitrogen (N) causing eutrophication-related phenomena in the coastal zones. As the N availability in receiving water bodies increases, excessive algal growth is stimulated and the eventual organic matter results in bottom water anoxia and cascading effects such as biodiversity loss, and alterations in food web structure and function [1,2]. At the same time, riverine sediments are active sites for biogeochemical reactions, such as denitrification, which acts as a natural buffer against nitrate (NO_3^-) pollution [3,4]. Denitrification, the stepwise reduction of NO_3^- to nitrogen gas (N_2) under anaerobic conditions, is widely recognized as the dominant biogeochemical process responsible for permanent N removal in rivers and transitional environments [5–7]. Anammox, the anaerobic oxidation of ammonium, can also remove inorganic N by combining ammonium (NH_4^+) with nitrite (NO_2^-) and releasing N_2; however, its occurrence is generally irrelevant if compared to denitrification in freshwater sediments [8,9].

Spatially distributed global models have demonstrated that denitrification occurring in river networks may remove, on average, 20–50% of the total land-based N input, indicating they are important filters for the N loadings transported toward the sea and therefore play a considerable role in mitigating eutrophication effects [7,10]. Although the denitrification capacity of the river networks has been recognized, most studies on the regulation of denitrification have addressed headwater streams because of their intense water–streambed interactions (i.e., a high ratio between bioreactive surfaces and water

volumes), sustaining significant in-stream N retention [11,12]. The nitrate (NO_3^-) supply to the benthic compartment is mainly controlled by diffusion from the water column; thus, N loss may decline with increasing channel size and depth because of less contact and exchange, making the denitrification process progressively less effective [13]. However, lowland rivers, deltas, and estuaries of agricultural basins in temperate zones may be ideal sites for denitrification, showing the typical features of eutrophic environments, such as elevated NO_3^- concentrations in water, organic carbon availability, and favorable temperatures during the spring–summer period [7,14,15]. Conversely, salinity increase along the river–sea gradient has been demonstrated to inhibit the denitrification activity of the sediments [16,17].

In eutrophic deltas, reduced flow and water mixing during the summer, concomitant with the establishment of steep thermal and/or saline gradients, may lead to partial or full stratification. Under these conditions, discriminating the source of NO_3^- fueling sedimentary denitrification, from the water column or nitrified at the water/sediment interface, is crucial for understanding benthic N metabolism [10]. Moreover, hypoxic or anoxic conditions may be established more frequently in stratified bottom waters, where NH_4^+ released from the sediments is not oxidized to NO_3^- and may accumulate [18,19].

The Po River Basin (Northern Italy) is one of the most densely populated and agriculturally exploited areas in Europe and is a well-known hotspot of eutrophication and NO_3^- pollution. Although several studies have addressed the N cycle in a wide variety of aquatic ecosystems in the basin, such as drainage canals, wetlands, lakes, and brackish coastal lagoons (e.g., [20–23]), the fate of the Po River N loadings through the delta remains unknown as they are measured at the closure of the basin, which is approximately 60 km upstream from the delta and more than 90 km from the outlet into the Adriatic Sea. Determining the factors controlling denitrification in lowland rivers and deltas is a crucial step in efforts to protect coastal zones from eutrophication caused by N excess. The quantitative relevance of denitrification in attenuating in-stream N loading during the season most sensitive to eutrophication has not been well established.

The aims of the present study were (i) to measure benthic denitrification in the Po River branch, namely the Po di Goro, taken as a case study representative of the other deltaic branches; (ii) to study the effect of water stratification along a 30 km salinity gradient, from the full riverine reach to the mouth to the sea; and (iii) to assess the role of denitrification in buffering N loadings to the Adriatic Sea in summer, the most sensitive period for eutrophication.

2. Materials and Methods

2.1. Study Area

The study area was the southernmost arm of the Po River Delta, named Po di Goro River, crossing northeast Italy for over 48 km, marking the borderline between the Emilia-Romagna and Veneto regions (Figure 1) The average annual discharge of the Po di Goro accounts for approximately 5% of the Po River discharge measured at Pontelagoscuro, more than 90 km upstream of the main river mouth and conventionally considered the basin closing section [24]. The Po di Goro River is partly connected to the Goro lagoon in its lower reach till the mouth to the Adriatic Sea. The Sacca di Goro, a shallow coastal lagoon, has suffered in the past from eutrophication, macroalgal blooms followed by summer anoxia, dystrophic crises, and massive deaths of farmed mollusks [25]. Freshwater and saltwater stratification and partial mixing are typical summer phenomena in the terminal Po di Goro River [26]. In recent years, an increase in salt intrusion has been detected in the lower Po di Goro River. For instance, the monitoring network of the Regional Environmental Protection Agency of the Emilia-Romagna region (ARPAE) has evidenced in summer a mean saltwater intrusion of approximately 13 km from the mouth to the sea.
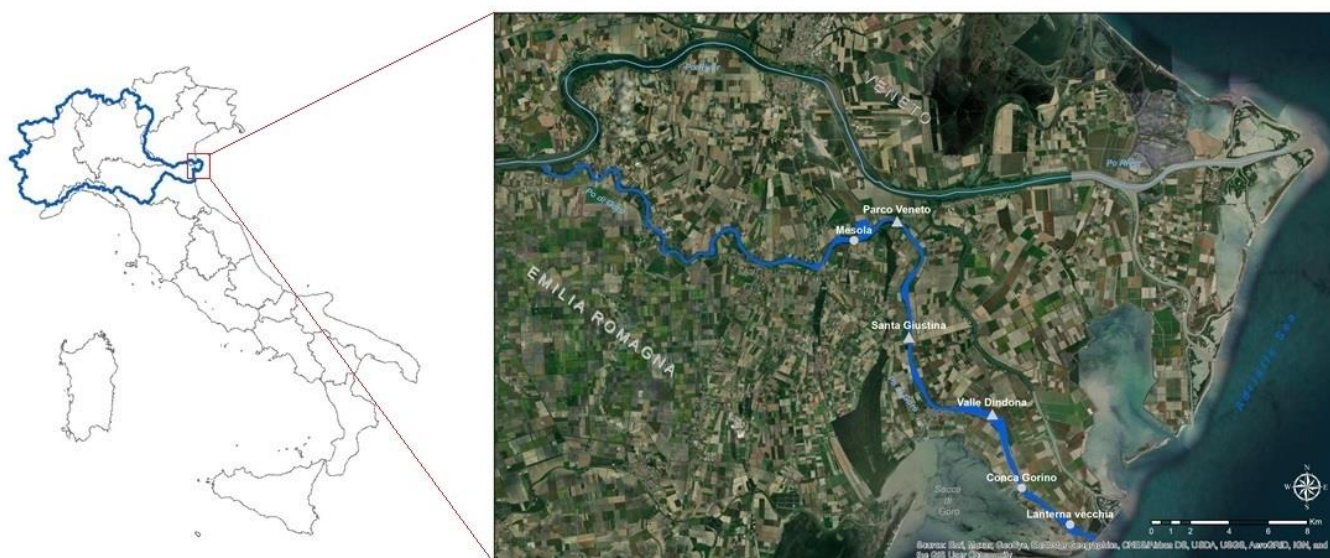
Figure 1. Study area. Location of the Po di Goro arm in Italy with the Po River Basin border reported in dark blue (map on the left). In the map on the right, the blue line represents the Po di Goro course and in light blue is indicated the Po River. Grey bubbles are the main study sites where sediment cores were sampled; while grey triangles indicate other monitoring stations along the Po di Goro (modified from basemap of ArcMap, ArcGIS 10.2.2., ESRI, Redlands, California).

In the present study, intact sediment cores were sampled in middle summer (end of July 2021) at three sections of the Po di Goro River along a salinity gradient: Mesola (M, 44°56′04.1′′ N and 12°15′03.9′′ E), Conca Gorino (G, 44°49′02.9′′ N and 12°21′11.3′′ E), and Lanterna Vecchia (LV, 44°47′59.0′′ N and 12°23′00.3′′ E), located 25, 5, and 1.5 km upstream, respectively, from the outlet into the Adriatic Sea (Figure 1; Table 1). The study area covered an overall surface of 7 km^2, and the three stations showed different characteristics. The M site was fully freshwater (340 μS cm^{-1}), the water column was thoroughly mixed, and the NO_3^- concentration (~90 μM) showed summer values typical of the terminal reach of the Po River [27]. At the bottom of G site, water was slightly saline, up to 11.2 ppt, while complete water stratification occurred at LV. In fact, in LV surface water, salinity was ~0.8 ppt and in depth ~18.1 ppt, due to salt intrusion from the Adriatic Sea. Nitrate availability decreased from ~60 μM to ~40 μM moving from G to LV (Table 1). During the sediment sampling campaign, profiles of physicochemical water variables (temperature, oxygen, electrical conductivity, and salinity) were monitored at different stations along the river course, demonstrating that freshwater conditions along the entire water depth extend from the M site to the location named Valle Dindona located approximately 5 km upstream from the G site.

Table 1. Features of the three sampling sites during the July campaign. Values of the bottom waters are reported.

Site	Distance from the Outlet (km)	Salinity (ppt)	NO_3^- (μM)	NH_4^+ (μM)	Total N (μM)
Mesola (M)	25	0.2	90	3	115
Conca Gorino (G)	5	11.2	59	13	122
Lanterna Vecchia (LV)	1.5	18.1	44	5	113

2.2. Sediment and Water Sampling

Measurements of sedimentary features, sediment oxygen demand, inorganic N fluxes (NO_3^-, NH_4^+, and N_2), and denitrification rates at the three sampling sites were performed in middle summer. Sampling and pre-incubation were performed according to standard-

ized procedures [28]. The experimental design consisted of the collection of seven intact sediment cores (plexiglass liners, internal diameter 4.5 cm, length 20 cm) at each site, of which five replicates were used for dark flux and denitrification measurements, and two replicates for sediment characterization. Only cores with visually undisturbed sediments and clear overlying water were used for further treatment. The sediment level of the collected intact cores was adjusted to approximately 9 cm on average, leaving an overlying water column of approximately 8 cm. Water column parameters (temperature, oxygen content, electrical conductivity, and salinity) were measured in situ with a multiparametric probe (YSI Model 85—Handheld Dissolved Oxygen, Conductivity, Salinity and Temperature System, YSI, Incorporated, Yellow Springs, OH, USA). After collection, the sediment cores were submerged in three different tanks with site water continuously aerated with aquarium pumps, and they were transported to the laboratory within a few hours. At each site, approximately 60 **L** of bottom water were collected using a Van Dorn bottle and brought to the laboratory for core maintenance, pre-incubation, and incubation periods.

2.3. Measurement of Benthic Fluxes and Denitrification Rates

In the laboratory, the sediment cores were maintained with the top open and aerated overnight in the dark. Each core was equipped with a Teflon-coated magnet, driven by a central magnet rotating at 40 rpm, which was suspended a few centimeters above the sediment surface to mix the water column while avoiding resuspension (Figure 2a,b). Water was stirred throughout the whole pre-incubation and incubation periods. Intact sediment cores were incubated in a batch mode according to standardized protocols developed for the measurement of benthic fluxes of gases and nutrients [28,29]. Incubations were performed in the laboratory at 25 °C, simulating the typical middle summer conditions in the Po River Delta. Dark fluxes of dissolved O_2 (SOD, sediment oxygen demand) and dissolved inorganic N (N_2, NO_3^-, NO_2^-, NH_4^+) across the water–sediment interface were quantified via start–end incubations lasting 2 h in order to maintain O_2 concentration within 20% of initial value [28]. Light penetration is generally very limited where the turbidity is high, such as in the Po River Delta; thus, the benthic compartment is assumed always to be in the dark. After overnight pre-incubation, five cores from each site were incubated in the dark. The water inside each tank was replaced with fresh water from each site in order to maintain near in situ dissolved nutrient concentrations. To initiate incubation, the water level in the tanks was lowered a few centimeters below the top of the cores and each liner was sealed with a rubber lid. Temperature and O_2 concentrations were measured with a multiparametric probe directly inside each core at the beginning and end of the incubation period. Simultaneously, water samples were collected from each core with a glass 60 mL syringe, filtered through Whatman GF/F glass fiber filters and transferred to polyethylene vials to analyze dissolved inorganic N compounds. In addition, samples for N_2:Ar were collected, transferred into 12 mL glass-tight vials (Exetainer, Labco, High Wycombe, UK) allowing abundant overflow, and preserved by adding 100 µL of 7 M $ZnCl_2$ to stop microbial activity. After the first incubation, the water in the tanks was replaced and the cores were submerged for approximately 1 h to stabilize. The isotope pairing technique (IPT [28,30]) was applied to measure denitrification rates on the same set of cores used for benthic flux determinations. At the beginning of the incubation, the water level in the tank was lowered just below the top of the cores, and aliquots of a stock solution of 15 mM $^{15}NO_3^-$ ($Na^{15}NO_3$, Sigma Aldrich) were added to the cores to obtain a final labelled NO_3^- enrichment of approximately 50%. The IPT incubation lasted 2 h from when the cores were capped. The NO_3^- concentrations were measured in each core before and after the addition of $^{15}NO_3^-$ to calculate the ^{14}N:^{15}N ratio in the NO_3^- pool. At the end of the incubation period, the entire sediment column was mixed with the water column to homogenize the dissolved N_2 pools in the water column and porewater. An aliquot of the slurry was transferred to a 12 mL Exetainer and fixed with 200 µL of 7 M $ZnCl_2$.
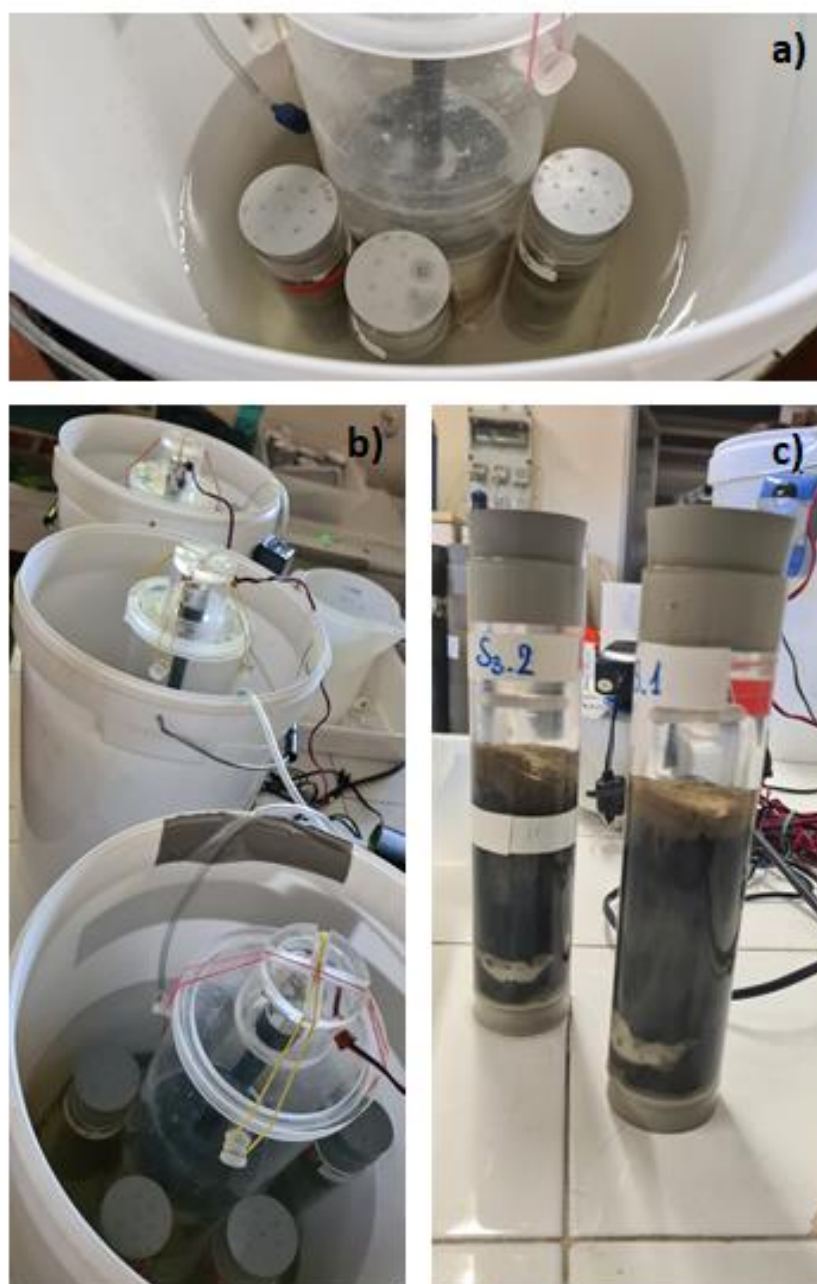
Figure 2. Laboratory design: (**a**) laboratory tank of one experimental site with sampling cores and central motor with mounted magnets to drive the individual magnetic stirrers within the cores; (**b**) experimental setup of the three sampling sites, consisting of five cores for each tank; (**c**) examples of sampling cores used for sediments characterization.

2.4. Analytical Methods, Calculation of Benthic Fluxes and Denitrification Rates

NO_2^- and NH_4^+ were analyzed via standard spectrophotometric methods using a Jasco V-550 spectrophotometer. NO_2^- was determined using sulfanilamide and N-(1-naphtyl)-ethylenediamine (detection limit 0.1 μM [31]). NH_4^+ was analyzed using salicylate and hypochlorite in the presence of sodium nitroprusside (detection limit 0.5 μM [32]). NO_3^- was analyzed using Technicon AutoAnalyser II (detection limit 0.4 μM [33]).

The N_2:Ar ratio (water samples from the incubation of benthic fluxes) and the abundance of $^{29}N_2$ and $^{30}N_2$ (slurry samples from the IPT incubation) were analyzed via membrane inlet mass spectrometry (MIMS) at the Laboratory of Aquatic Ecology, University of Ferrara (Bay instrument, MD, USA [34]). For MIMS analyses, the samples, after equilibra-

tion at 20 °C, were pumped through an under-vacuum gas-permeable silicone membrane. The extracted gases passed through (i) a liquid nitrogen cryogenic trap to remove carbon dioxide and water vapor, (ii) a copper reduction column controlled by a muffle furnace operating at 600 °C to remove oxygen, and finally (iii) a second liquid nitrogen trap before ionization and detection by a PrismaPlus quadrupole mass spectrometer [35,36]. The concentration of N_2 was calculated from the measured N_2:Ar ratio multiplied by the theoretical saturated Ar concentration at the sampling water temperature determined from gas solubility tables [37]. Benthic N_2 fluxes include coupled nitrification/denitrification and anammox. However, several studies showed that contribution of anammox to N_2 production in organic-rich freshwater ecosystems is generally negligible [3,38,39].

Dark fluxes were calculated from the rate of change in concentrations with time, according to the following equation [29]:

$$F_x = \frac{(C_0 - C_f) \cdot V}{A \cdot t}$$

where F_x (μmol m^{-2} h^{-1}) is the flux of a general compound, C_0 and C_f (μM) are the concentrations of the compound at the beginning and the end of incubation, respectively, V (L) is the water volume of the core, A (m^2) is the area of the sediment core, and t (h) is the time of incubation. Negative values indicate fluxes from the water column to the sediment, whereas positive values indicate fluxes from sediment to the water column.

Denitrification rates were calculated as described by [29]:

$$D_{15} = p29 + 2p30 \quad D_{14} = D_{15} \cdot \left(\frac{p29}{2p30} \right)$$

where D_{15} is the denitrification rate of the added $^{15}NO_3{}^-$, D_{14} is the total denitrification rate of $^{14}NO_3{}^-$, and p29 and p30 are the production rates of $^{29}N_2$ and $^{30}N_2$, respectively. The denitrification of $NO_3{}^-$ diffusing to the anoxic sediment layer from the water column (D_w) and the denitrification of $NO_3{}^-$ produced within the oxic sediment layer by nitrification (Dn) were calculated according to [30]:

$$D_w = \frac{^{14}NO_3^-}{^{15}NO_3^-} \cdot D_{15} \quad D_n = D_{14} - D_w$$

where $^{14}NO_3{}^-$ is the ambient nitrate and $^{15}NO_3{}^-$ is the labelled nitrate added to each core.

2.5. Sediment Characterization

The cores for sediment characterization (Figure 2c) were processed as follows. The upper 0–1 cm section was sliced, and rapidly homogenized and sediment subsamples of 5 mL were used to determine the physical properties. Bulk density was determined as the ratio of wet weight to volume. Porosity and water content (%) were determined from weight loss of a known fresh sediment volume, after drying at 50 °C to constant weight for 72 h. Finally, the dried samples (approximately 0.5 g) were placed into a muffle furnace at 350 °C for 3 h to quantify the organic matter content (OM, %), based on the weight loss by ignition.

2.6. Riverine N Loadings in the Po di Goro and Importance of $NO_3{}^-$ Removal via Denitrification

Daily total N loadings transported by the Po di Goro River to the Adriatic Sea in the middle summer (July and August) months were calculated using official concentration and discharge datasets collected for the period 2014–2019. Nitrogen species concentrations were obtained by monthly sampling campaigns carried out at the Serravalle station (44°58′43.6″ N and 11°59′51.9″ E) in the framework of the ARPAE environmental monitoring program (https://dati.arpae.it/, accessed on 23 October 2021). The station is located on the main course of the Po River just before the diversion of the Po di Goro branch.

Sample collection and analysis were performed in accordance with standard methods and analytical protocols [40]. The daily average discharges of the Po River (Pontelagoscuro station, 44°53′19.34″ N and 11°36′29.60″ E) were acquired from the permanent records of a gauge operated by ARPAE. Discharge datasets were retrieved from the "Hydrological Annals—Second Part" published by ARPAE and available on the Regional Open Data Portal (https://simc.arpae.it/dext3r/, accessed on 23 October 2021). The discharge of the Po di Goro River was calculated as a function of the discharge measured at Pontelagoscuro by employing a predictive experimental equation obtained from data reviewed by the Environmental Agency of the Veneto Region (Supplementary Materials, Figure S1). Daily total N loadings were calculated by multiplying monthly concentrations by average monthly discharge and compared to the amount potentially removed by the entire sampled reach of the Po di Goro River obtained by scaling up the experimentally measured denitrification rates. The proportion of the N amount removed in the reach versus the total N loading entering that reach was considered as the denitrification efficiency.

2.7. Statistical Analysis

Differences among the three sampling sites in inorganic N fluxes, denitrification rates and SOD measured by core incubations were tested via one-way ANOVA and pairwise multiple comparisons of means (post hoc test, Tukey's test). Normality (Shapiro–Wilk test) and homoscedasticity (Levene's test) were examined, and all datasets fulfilled the requirements for parametric tests. Statistical analysis was performed using SigmaPlot 11.0 (Systat Software, Inc., San Jose, CA, USA), and the overall significance level was set at $p \leq 0.05$.

3. Results and Discussion

3.1. Factors Controlling NO_3^- Removal via Denitrification in the Po di Goro Sediments

Nitrate fluxes were always negative, indicating that consumption from the overlying bottom water occurred in the sediments of the Po di Goro River owing to benthic processes (Figure 3a). Nitrate removal rates differed among sampling sites (Table 1), with higher values at M and G sites (on average -402 ± 169 and -397 ± 193 μmol N m^{-2} h^{-1}, respectively) than at LV site (-83 ± 41 μmol N m^{-2} h^{-1}), reflecting a decrease in water NO_3^- availability along the river–sea gradient from the fully riverine reach (~90 μM) to the outlet into the Adriatic Sea (~40 μM). Similarly, the N_2 fluxes and Dtot and Dw rates were significantly different among the three sampling sites (Figure 3a, Table 2). The highest Dtot rates were measured at the M site and were almost equivalent to the rates of N_2 production and NO_3^- consumption (422 ± 99 and -424 ± 103 μmol N m^{-2} h^{-1}, respectively), exceeding, by a factor of four on average, the rates measured at LV, the site nearest to the sea. At LV, the lowest NO_3^- availability in the water resulted in the lowest rates of N_2 production and Dtot measured for the Po di Goro sediments. The post hoc Tukey's test showed significant differences in N fluxes (NO_3^- and N_2) and denitrification rates between M and LV and between G and LV sites, but not between M and G sites (Table 2).

Nitrate fluxes measured in single cores sampled from the Po di Goro River ranged between -640 μmol N m^{-2} h^{-1} and -48 μmol N m^{-2} h^{-1} and were highly correlated with both Dw rates ($p < 0.0001$) and N_2 effluxes ($p < 0.0001$) (Figure 3b,d; Table S2). The highest consumption of NO_3^- corresponded to the highest Dw rates and also to the maximum rates of N_2 production (Figure 3b,d). The generally good correlation between NO_3^- demand and N_2 effluxes detected in all the sampled sites demonstrated that denitrification was the main process responsible for reactive N removal and was quantitatively fueled by water column NO_3^-. Anammox cannot be excluded to occur and partially contribute to N_2 effluxes. However, studies measuring denitrification and anammox simultaneously in eutrophic and organic-rich freshwater ecosystems demonstrated that the contribution of anammox to the total N_2 production was generally <10% [3,38,39], and summer appeared to be a relatively unfavorable season for anammox bacterial growth [41].
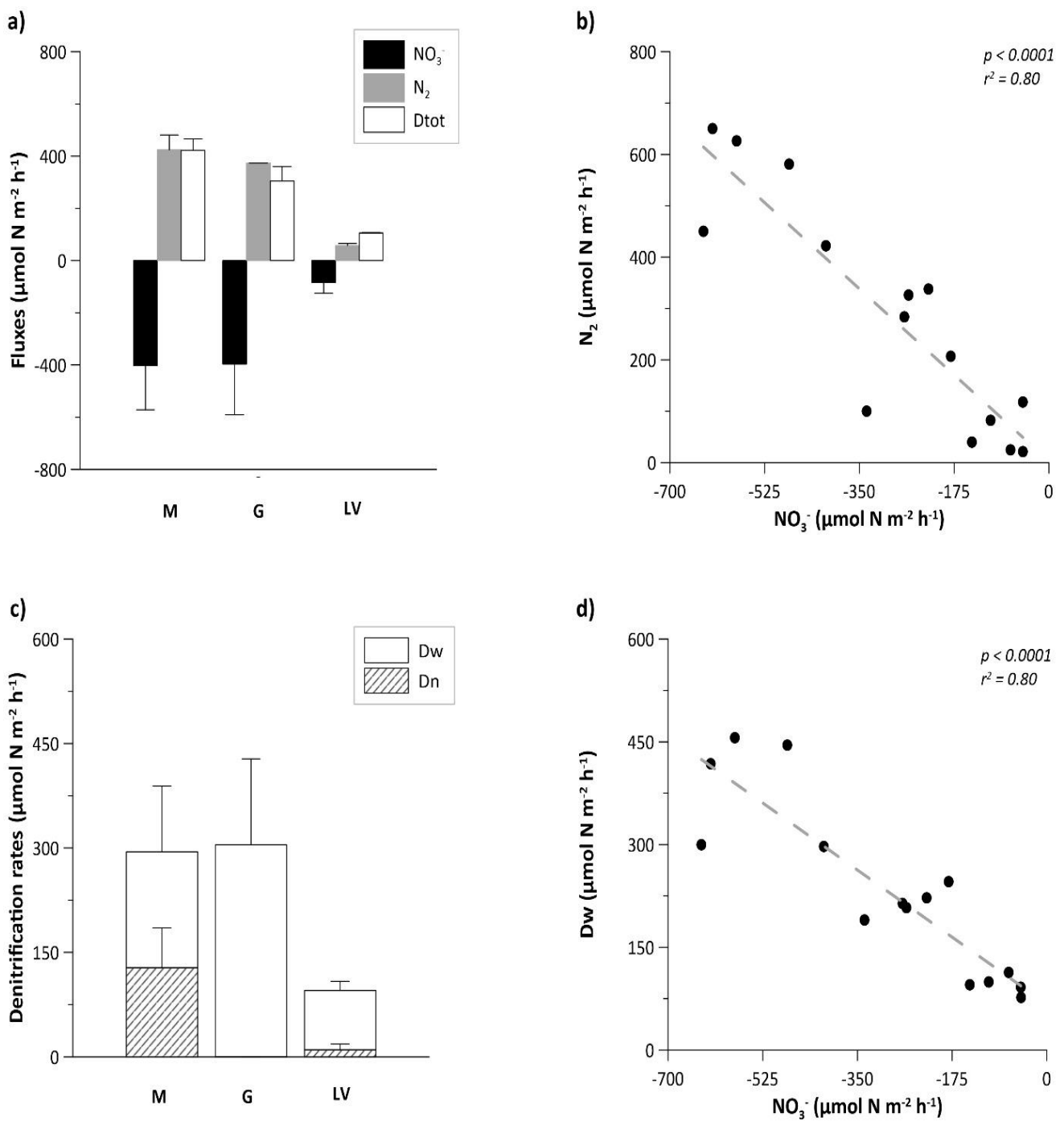
Figure 3. Benthic dark fluxes of inorganic N measured at the three sampling sites. (**a**) Fluxes of NO_3^- and N_2, and total denitrification (Dtot), (**b**) relation between fluxes of NO_3^- and N_2, (**c**) denitrification rates split into denitrification of water column NO_3^- (Dw, white bars) and denitrification coupled to nitrification in the sediment (Dn, hatched bars), (**d**) relation between fluxes of NO_3^- and Dw. In panels (**a,c**), average values ± standard deviations are reported, while graphs of panels (**b,d**) include single core measurements.

Table 2. Results of the one-way ANOVA and Tukey's test ($p < 0.05$). NS = not statistically significant.

Parameter	p	F	Turkey's Test
Dtot	<0.001	15.45	M vs. LV G vs. LV
Dw	<0.01	8.65	M vs. LV G vs. LV
NO_3^- flux	<0.01	7.37	M vs. LV G vs. LV
N_2 flux	<0.01	7.88	M vs. LV G vs. LV
NH_4^+ flux	NS	2.82	-
SOD	NS	0.68	-

In the Po di Goro sediment, denitrification was stimulated when NO_3^- availability in the water was greater (M) and the sediment richer in OM (G), whereas it was inhibited at the most saline site (LV). The highest rates measured at M and G reflected the occurrence of the three primary controls directly influencing denitrification, that is, availability of NO_3^- and organic carbon and anoxic environment. Nitrate and organic carbon availability, acting as terminal electron acceptor and electron supplier for denitrifying bacteria, respectively, are generally considered as the most important drivers determining the magnitude of denitrification [42]. The present outcomes were consistent with studies performed in a vast array of aquatic ecosystems demonstrating that high concentrations of NO_3^- and interstitially dissolved organic carbon, as well as low oxygen levels, in the overlying water enhance denitrification in summer [6,43]. Although NO_3^- concentrations decreased from M to G, the total denitrification rates were similar, likely resulting from a combination of factors, that is, the stimulating effect of higher sediment OM occurring at G (Table 3) together with the salinity-induced stratification. Low oxygen concentrations in the water column stimulate denitrification by reducing the distance for NO_3^- diffusion to encounter anoxic conditions in the sediment. The higher availability of labile OM occurring at G was likely a consequence of salinity-induced flocculation of the particulate organic load [44]. Sediment organic enrichment stimulates denitrification directly by providing an energy source for heterotrophic denitrifying bacteria, as well as indirectly, by fueling respiration that depletes dissolved oxygen in the benthic compartment [5,45]. A higher SOD value (~3100 μmol O_2 m^{-2} h^{-1}) appeared at G, indicating muddy–sandy sediments rich in OM (4.2%), while lower rates of oxygen consumption (~2700 μmol O_2 m^{-2} h^{-1}) were measured in sediments with lower organic enrichments (Table 3; Figure 4a; Table S2). No significant differences in SOD were observed among the sampling sites, but they overall resulted in a higher range of rates reported in the literature for freshwater eutrophic environments [21,46–48].

Table 3. Sediment characteristics at the three sampling sites of the Po di Goro River. Average values $\pm$ standard deviations are reported.

	M	G	LV
Typology	sandy	muddy–sandy	clay
Porosity	0.63 ± 0.08	0.64 ± 0.12	0.51 ± 0.04
Density (g/mL)	1.56 ± 0.17	1.14 ± 0.18	1.41 ± 0.32
OM (%)	2.00 ± 1.00	4.30 ± 0.40	1.80 ± 0.00

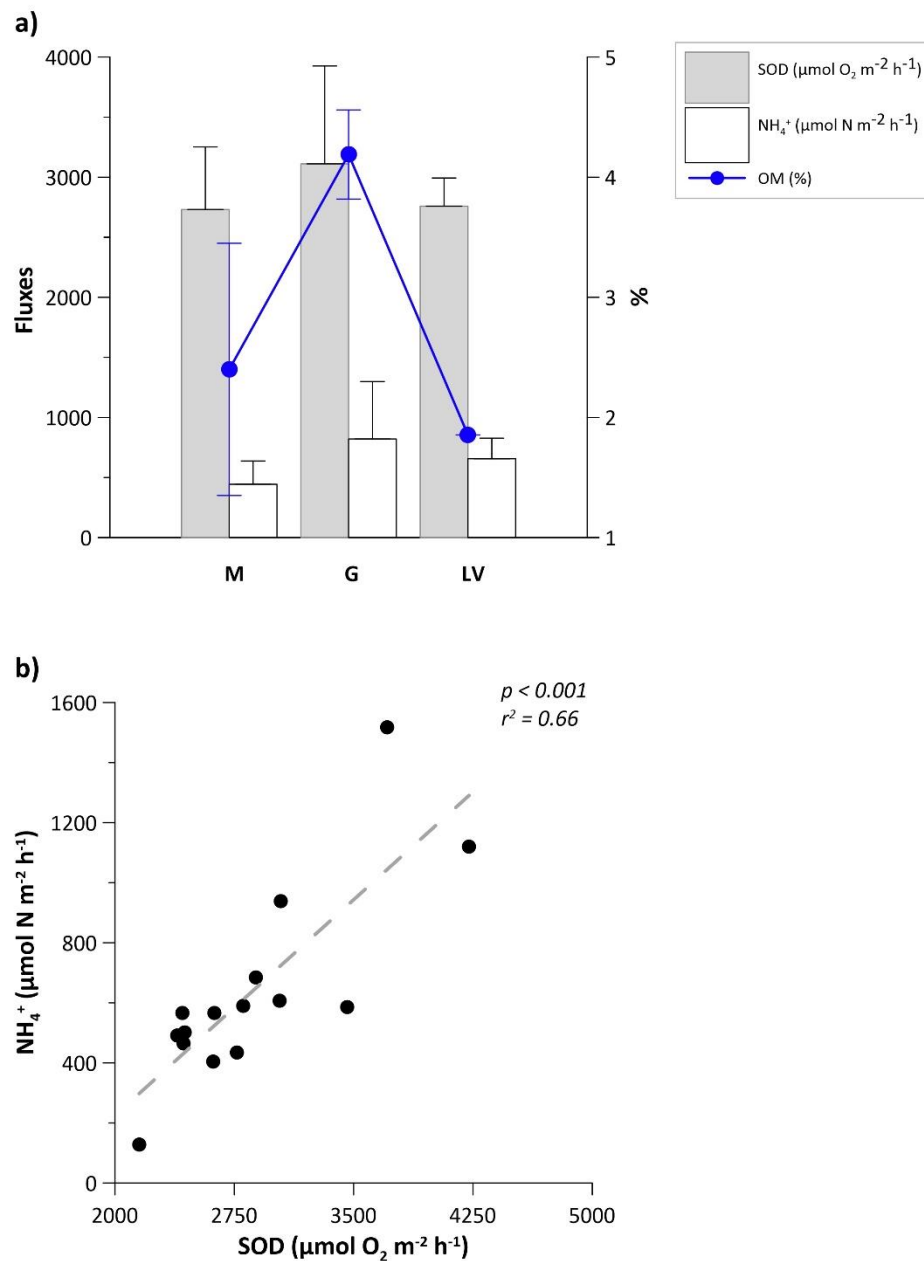**Figure 4.** (**a**) Benthic dark fluxes of oxygen and NH_4^+ and sediment OM measured at the three sampling sites, (**b**) relation between dark oxygen fluxes and NH_4^+ fluxes. In panel (**a**), average values ± standard deviations are reported, while the graph of panel (**b**) includes single core measurements.

Denitrification supported by water column NO_3^- contributed mostly (70–100%) to total rates, as widely reported in the literature when water NO_3^- concentrations exceed 50−60 μM [10,21]. At all sites, sediments were simultaneously a net sink of water column NO_3^- but also a source of NH_4^+. Ammonium fluxes were always positive, indicating a production in the benthic compartment and a release to the overlying bottom water as a consequence of OM mineralization (Figure 4b; Table S2). The generally good correlation between NO_3^- and N_2 effluxes, and Dw rates (Figure 3) demonstrated that denitrification was the main process responsible for NO_3^- consumption. Dissimilatory nitrate reduction to ammonium (DNRA) cannot be excluded as a process contributing partially to NH_4^+ recycling from the sediment, especially in those sites with a higher ratio between sedimentary organic carbon and water column NO_3^-, such as G and LV. Previous studies have

demonstrated that reducing (sulfidic) conditions, such as those established in OM-rich sites, do favor DNRA over denitrification [48–50].

Denitrification coupled to nitrification was likely controlled by the limited oxygen availability at the sediment–water interface, preventing NH_4^+ oxidation, occurring as a consequence of water stratification, a typical summer condition of lowland canalized rivers and transitional environments [26,51,52]. At the G site, the bottom water was the dominant source of nitrate, accounting for 100% of the total amount required for denitrification. Here, the mineralization of the high OM content reduced the oxygen availability into the sediments, creating the anoxic conditions that prevented coupled nitrification–denitrification [48,53,54]. Conversely, coupled nitrification–denitrification was the highest at M (~130 μmol N m^{-2} h^{-1}, Figure 3c; Table S2), accounting for ~30% of the total denitrification rate, reflecting the thorough mixing of the water column and the oxygenation of the surface sediment. At the LV site, the denitrification rate was the lowest, because of the concomitant low water NO_3^- availability, increased salinity, and permanent stratification resulting in anoxic conditions in the benthic compartment. Salinity has been demonstrated to place physiological stress on bacterial communities, such as nitrifiers and denitrifiers [18]. In the sediments of transitional environments, the depletion of electron acceptors such as O_2 and NO_3^- generally leads to the dominance of sulphate reduction as a decomposition pathway accounting for a large part of the organic matter oxidation. Persistent anoxia is thus accompanied by a significant release of sulfide to the water column, a condition inhibiting nitrification and denitrification [55]. Organic enrichment and reducing conditions under persistent stratification may shift NO_3^- reduction towards more pronounced DNRA, with internal NO_3^- recycling to NH_4^+. Future research should address the concomitant measurement of denitrification and DNRA in deltaic environments to better understand the balance between N removal and N recycling processes.

3.2. Denitrification Rates in the Po di Goro: Comparison to the Literature and Relevance in Attenuating the Riverine N Loadings in Summer

The denitrification rates measured in the Po di Goro sediments were in line with those reported in the literature for estuarine and delta systems around the world with water temperatures > 20 °C (Table 4). The observed high spatial variability is typical of transitional zones where a multitude of factors are in a constant state of change, such as NO_3^- supply, rates of organic carbon sedimentation, and redox condition in the overlying water and surface sediments. The rates measured in this study for the freshwater site (M) were higher than the range of observations for nonsaline locations of other estuarine and delta systems (Table 4). This discrepancy is most likely due to the presence of a mixed NO_3^--rich water column which ensures a constant supply of NO_3^- to the benthic bioreactive surfaces where denitrification occurs. A combination of salinity-induced stratification and NO_3^- decrease plays a role in reducing the denitrification capacity along the river–sea gradient, as previously observed for other transitional environments [14,56].

In a worldwide hotspot of eutrophication and NO_3^- pollution, such as the Po River Basin, denitrification has been widely measured in several aquatic ecosystem types (e.g., wetlands, canals, lagoons, lakes), and its controlling factors diffusively investigated, resulting in the main process responsible for reactive N removal, especially in freshwater environments [20–22]. A comprehensive summary of denitrification measurements performed in the aquatic ecosystems of the Po River Basin during the summer period is presented in Figure 5. Details of the sampling locations and the main sediment and water features are reported in the Supplementary Material (Table S1). Summer denitrification was quite different among aquatic ecosystem types, with measured rates spanning along three orders of magnitude, i.e., from <2 to ~2000 μmol N m^{-2} h^{-1}. On average, the highest denitrification rates were found in aquatic environments tightly linked to the surrounding agricultural landscapes (connected wetlands and rivers), resulting in an increased availability of NO_3^- and labile organic carbon (Figure 5). The range of denitrification rates measured in the Po di Goro sediments overlapped with estimates of denitrification in

connected wetlands and rivers of the Po River Basin and was higher than those found in isolated wetlands, lakes, and coastal lagoons. Generally, denitrification rates were supported mainly by Dw in all aquatic ecosystems, with only the exception of lagoons, where sediment oxidation mediated by bioturbation contributes to stimulating coupled nitrification-denitrification [23].
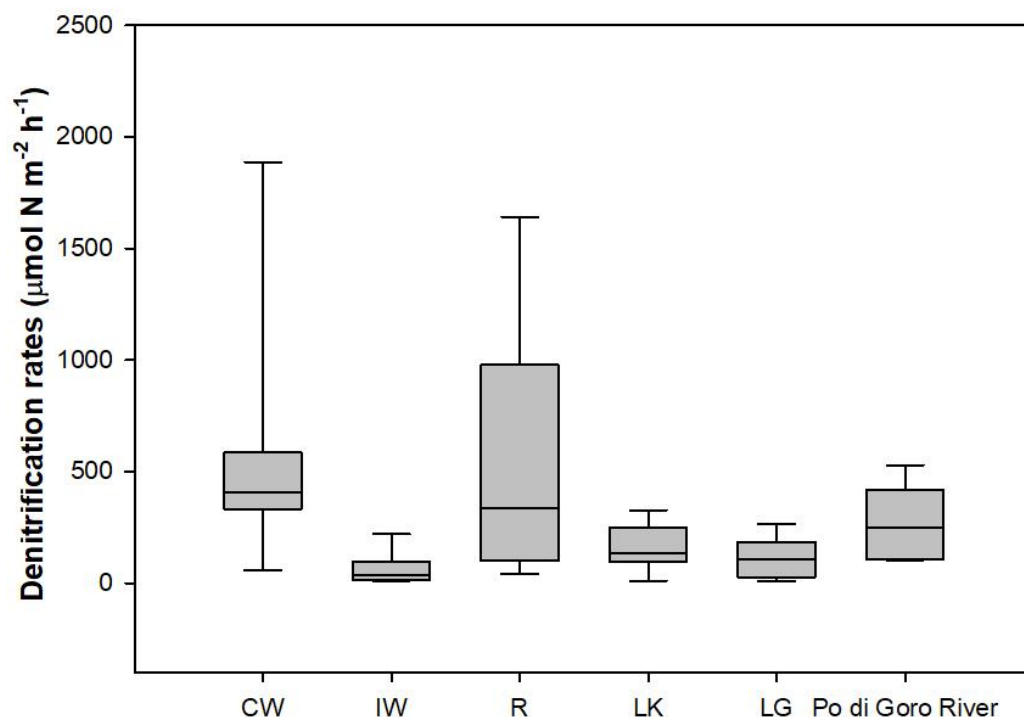

Figure 5. Boxplot on total denitrification rates measured during the period of highest temperature of the year in different aquatic ecosystems of the Po River Basin (CW, connected wetlands; IW, isolated wetlands; R, rivers; LK, lakes; LG, lagoons). The central horizontal line in the box is the median, the top and bottom boxes are 25th and 75th percentiles, and the whiskers are 10th and 90th percentiles. The employed datasets are reported in Table S1 (Supplementary Material).

Denitrification rates in the Po di Goro sediments can be addressed in a mass balance context to assess the relevance of the process at the whole-reach scale. Daily TN loadings transported by the Po di Goro River to the Adriatic Sea in middle summer varied between 1.6 and 4.8 t N day^{-1} according to different discharge values (13–35 m^3 s^{-1}) and NO_3^- was the dominant nitrogen form (on average 76–86% of TN). By extrapolating the total denitrification rates measured by sediment core incubations, the whole Po di Goro sampled reach ($\sim$7 km^2) was estimated to potentially dissipate by denitrification up to 0.94 $\pm$ 0.23 t N day^{-1}. Despite different drivers regulating denitrification at the three sampling sites, the present outcomes demonstrated that, in middle summer conditions, deltaic denitrification may remove a significant fraction, on average 28%, of the TN load transported by the Po di Goro to the Adriatic Sea, highlighting a previously underestimated role of the Po River terminal arms. Studies performed in several transitional environments around the world have estimated highly variable denitrification efficiency, contributing to removing from <10% to $\sim$50% of the annual N loading (e.g., [57–59]). However, the rate at which this process occurs and how it affects the N supply to the coastal zones and the availability for primary producers is particularly important to address during summer periods when the eutrophication risk is higher. The present data suggest that the TN loadings, which are usually derived from river gauging above the tidal limit, overestimate, by nearly 30%, the real loadings reaching the Adriatic Sea in summer as they do not take into account the deltaic denitrification capacity. Quantitative information on N cycling in

deltaic sediments with high temporal and spatial resolution is needed to better understand how N loading from watersheds may affect eutrophication phenomena in the coastal zones.

Table 4. Total denitrification rates measured via isotope pairing technique in selected transitional environments (deltas and estuaries) around the world during the summer period. Main sediment and water features are reported for comparison with the results of this study. Standard deviations are reported.

Location	T (°C)	Salinity (‰)	NO_3^- (μM)	SOD (μmol O_2 m^{-2} h^{-1})	Dtot (μmol N m^{-2} h^{-1})	OM (%)	References
The Colne estuary (UK)	25	-	141	-	353 ± 37	-	[60]
Norsminde Fjord—shallow estuary (Denmark)	23	0.1–19.4	<1	-	106 ± 1		[61]
	23		2		153 ± 28	-	
Neuse River (North Carolina)	29		11	681 ± 88	8		[62]
	29		17	256 ± 177	73		
	26	-	24	647 ± 411	143		
	29		38	1187 ± 143	51	-	
	24.5		32	791 ± 136	19		
Wax Lake Delta (Louisiana)	30	0.1–0.4	58	1186 ± 143	41 ± 2	2	[15]
Barataria Bay (Louisiana)	30	0.1–0.4	45	1527 ± 451	42 ± 10	2	
Nueces River (Texas)	30	0.29	67	736 ± 2	27 ± 6	-	[63]
Corpus Christi Bay (Texas)	32.3	1.94	2	1077 ± 70	7 ± 1	-	
Thames estuary– Site 1 (UK)	-	2–32	611	3113 ± 184	4826 ± 395	4	[56]
Site 2	-	2–32	*	2884 ± 538	146 ± 28	2	
Site 3	-	2–32	*	5384 ± 186	140 ± 33	2	
Site 4	-	2–32	*	5486 ± 504	175 ± 55	3	
Site 5	-	2–32	*	4379 ± 914	462 ± 68	3	
Site 6	-	2–32	*	3680 ± 413	103 ± 9	1	
Wax Lake Delta (Louisiana)	27.3	0.2	64	1833	397	5	[64]
	19	0.2–0.4	98	1042 ± 0	115 ± 7	3	[14]
	22.2	0.2–0.4	102	1953 ±130	87 ± 5	6	
	21.2	0.2–0.4	82	3646 ± 130	230 ± 10	22	
Mildred Island (Suisun Delta, USA)	22.2	0.1	-	1160 ± 130	20	-	[19]
Franks (Suisun Delta, USA)	22	0.1	-	1490 ± 55	48 ± 3	-	
Big Break (Suisun Delta, USA)	21.5	0.1	-	1062 ± 32	21 ± 11	-	
Sherman Island (Suisun Delta, USA)	21	0.2	-	947 ± 98	71 ± 12	-	
Brown (Suisun Bay, USA)	21	0.4	-	1490 ± 250	53 ± 5	-	
Po di Goro (Mesola)	25	0.2	89	2731 ± 521	422 ± 99	2	This study
Po di Goro (Conca Gorino)	25	11.2	61	3111 ± 815	305 ± 123	4.3	
Po di Goro (Lanterna Vecchia)	25	18.1	71	2759 ± 234	105 ± 5	1.8	

* Nitrate concentration decreased along the river–sea gradient.

4. Conclusions

Benthic denitrification in the Po delta sediments was a net sink of N, which accounted for a significant reduction in TN loading to the coastal zone. These outcomes underscore the role of the terminal branches of the Po River delta, previously underestimated, as a buffering system as a whole, against summer N loadings and for the protection of coastal areas, right when eutrophication risk is the highest. Sedimentary regeneration of NH_4^+ was measured at all stations and partially counterbalanced N losses via denitrification. This positive

contribution to the generation of reactive N was unexpectedly high and requires further investigation. Knowledge of spatial and temporal variability and the relative importance of contrasting paths of the N cycle, such as denitrification and ammonia regeneration in deltaic sediments, is a key point for the definition of effective interventions to mitigating NO_3^- pollution and coastal eutrophication.

These preliminary findings need to be progressed both at the microscale (e.g., assessment of environmental drivers controlling benthic N dynamics) and at the whole-reach scale. Moreover, investigating the effects of increasing water temperature and saline intrusion on denitrification as consequences of global warming is of great interest for future studies on the buffering capacity against N loadings in deltaic ecosystems.

Supplementary Materials: The following are available online at https://www.mdpi.com/article/10.3390/w14030501/s1. Figure S1: Relation between the discharge (Q) of the Po River measured at Pontelagoscuro station and the percentage transported by the Po di Goro branch. Table S1: Total denitrification rates measured via isotope pairing technique in different aquatic ecosystems of the Po River Basin during the period of highest temperature of the year (CW, connected wetlands; IW, isolated wetlands; R, rivers; LK, lakes; LG, lagoons). Table S2: Summary of benthic fluxes and denitrification rates measured in the Po di Goro.

Author Contributions: Conceptualization, M.P.G., E.S. and G.C.; methodology, E.S. and G.C.; investigation, M.P.G., E.S., F.V. and G.C.; resources, F.V.; formal analysis, M.P.G.; writing—original draft preparation, M.P.G.; writing—review and editing, E.S. and G.C.; visualization, M.P.G.; funding acquisition, G.C.; supervision, G.C. All authors read and agreed to the published version of the manuscript.

Data Availability Statement: Data collected by the Regional Environmental Protection Agency of the Emilia-Romagna region are available online at https://dati.arpae.it/ and https://simc.arpae.it/dext3r.

Conflicts of Interest: The authors declare no conflict of interest.

References

1. Glibert, P.M.; Harrison, J.; Heil, C.; Seitzinger, S. Escalating worldwide use of urea–a global change contributing to coastal eutrophication. *Biogeochemistry* **2006**, *77*, 441–463. [CrossRef]
2. Howarth, R.W.; Marino, R. Nitrogen as the limiting nutrient for eutrophication in coastal marine ecosystems: Evolving views over three decades. *Limnol. Oceanogr.* **2006**, *51*, 364–376. [CrossRef]
3. Zhou, S.; Borjigin, S.; Riya, S.; Terada, A.; Hosomi, M. The relationship between anammox and denitrification in the sediment of an inland river. *Sci. Total Environ.* **2014**, *490*, 1029–1036. [CrossRef]
4. Li, J.; Yu, S.; Qin, S. Removal capacities and environmental constrains of denitrification and anammox processes in eutrophic riverine sediments. *Water Air Soil Pollut.* **2020**, *231*, 1–16. [CrossRef]
5. Cornwell, J.C.; Kemp, W.M.; Kana, T.M. Denitrification in coastal ecosystems: Methods, environmental controls, and ecosystem level controls, a review. *Aquat. Ecol.* **1999**, *33*, 41–54. [CrossRef]
6. Piña-Ochoa, E.; Álvarez-Cobelas, M. Denitrification in Aquatic Environments: A Cross-system Analysis. *Biogeochemistry* **2006**, *81*, 111–130. [CrossRef]
7. Birgand, F.; Skaggs, R.W.; Chescheir, G.M.; Gilliam, J.W. Nitrogen removal in streams of agricultural catchments—A literature review. *Crit. Rev. Environ. Sci. Technol.* **2007**, *37*, 381–487. [CrossRef]
8. Zhu, G.; Wang, S.; Zhou, L.; Wang, Y.; Zhao, S.; Xia, C.; Wang, W.; Zhou, R.; Wang, C.; Jetten, M.S.M.; et al. Ubiquitous anaerobic ammonium oxidation in inland waters of China: An overlooked nitrous oxide mitigation process. *Sci. Rep.* **2015**, *5*, 1–10. [CrossRef]

9. Chen, H.; Zhang, B.; Yu, C.; Zhang, Z.; Yao, J.; Jin, R. The effects of magnetite on anammox performance: Phenomena to mechanisms. *Bioresour. Technol.* **2021**, *337*, 125470. [CrossRef]

10. Seitzinger, S.; Harrison, J.A.; Böhlke, J.K.; Bouwman, A.F.; Lowrance, R.; Peterson, B.; Tobias, C.; Drecht, G.V. Denitrification across landscapes and waterscapes: A synthesis. *Ecol. Appl.* **2006**, *16*, 2064–2090. [CrossRef]

11. Peterson, B.J.; Wollheim, W.M.; Mulholland, P.J.; Webster, J.R.; Meyer, J.L.; Tank, J.L.; Martì, E.; Bowden, W.B.; Valett, H.M.; Hershey, A.E.; et al. Control of nitrogen export from watersheds by headwater streams. *Science* **2001**, *292*, 86–90. [CrossRef]

12. Herrman, K.S.; Bouchard, V.; Moore, R.H. Factors affecting denitrification in agricultural headwater streams in Northeast Ohio, USA. *Hydrobiologia* **2008**, *598*, 305–314. [CrossRef]

13. Alexander, R.B.; Smith, R.A.; Schwarz, G.E. Effect of stream channel size on the delivery of nitrogen to the Gulf of Mexico. *Nature* **2000**, *403*, 758–761. [CrossRef] [PubMed]

14. Li, S.; Twilley, R.R. Nitrogen dynamics of inundated sediments in an emerging coastal deltaic floodplain in mississippi river delta using isotope pairing technique to test response to nitrate enrichment and sediment organic matter. *Estuaries Coasts* **2021**, *44*, 1899–1915. [CrossRef]

15. Upreti, K.; Rivera-Monroy, V.H.; Maiti, K.; Giblin, A.; Geaghan, J.P. Emerging wetlands from river diversions can sustain high denitrification rates in a coastal delta. *J. Geophys. Res. Biogeosci.* **2021**, *126*, e2020JG006217. [CrossRef]

16. Seo, D.C.; Yu, K.; Delaune, R.D. Influence of salinity level on sediment denitrification in a Louisiana estuary receiving diverted Mississippi River water. *Arch. Agron. Soil Sci.* **2008**, *54*, 249–257. [CrossRef]

17. Giblin, A.E.; Weston, N.B.; Banta, G.T.; Tucker, J.; Hopkinson, C.S. The effects of salinity on nitrogen losses from an oligohaline estuarine sediment. *Estuaries Coasts* **2010**, *33*, 1054–1068. [CrossRef]

18. Rysgaard, S.; Thastum, P.; Dalsgaard, T.; Christensen, P.B.; Sloth, N.P. Effects of salinity on NH_4^+ adsorption capacity, nitrification, and denitrification in Danish estuarine sediments. *Estuaries* **1999**, *22*, 21–30. [CrossRef]

19. Cornwell, J.C.; Glibert, P.M.; Owens, M.S. Nutrient fluxes from sediments in the San Francisco Bay Delta. *Estuaries Coasts* **2014**, *37*, 1120–1133. [CrossRef]

20. Pinardi, M.; Bartoli, M.; Longhi, D.; Viaroli, P. Net autotrophy in a fluvial lake: The relative role of phytoplankton and floating-leaved macrophytes. *Aquat. Sci.* **2011**, *73*, 389–403. [CrossRef]

21. Racchetti, E.; Bartoli, M.; Soana, E.; Longhi, D.; Christian, R.R.; Pinardi, M.; Viaroli, P. Influence of hydrological connectivity of riverine wetlands on nitrogen removal via denitrification. *Biogeochemistry* **2011**, *103*, 335–354. [CrossRef]

22. Castaldelli, G.; Soana, E.; Racchetti, E.; Vincenzi, F.; Fano, E.A.; Bartoli, M. Vegetated canals mitigate nitrogen surplus in agricultural watersheds. *Agric. Ecosyst. Environ.* **2015**, *212*, 253–262. [CrossRef]

23. Magri, M.; Benelli, S.; Bonaglia, S.; Zilius, M.; Castaldelli, G.; Bartoli, M. The effects of hydrological extremes on denitrification, dissimilatory nitrate reduction to ammonium (DNRA) and mineralization in a coastal lagoon. *Sci. Total Environ.* **2020**, *740*, 140169. [CrossRef] [PubMed]

24. Environmental Protection Agency of the Veneto Region. Distribution of Flows Among the Branches of the Po River and the outlets of the Po Delta Po: Historical Experiences and New Investigations During the 2011. Relation n° 2/12. In Italian. 2012. Available online: https://www.arpa.veneto.it/temi-ambientali/idrologia/approfondimenti/lidrologia-del-delta-del-po (accessed on 23 October 2021).

25. Viaroli, P.; Giordani, G.; Bartoli, M.; Naldi, M.; Azzoni, R.; Nizzoli, D.; Ferrari, I.; Comenges, J.M.Z.; Bencivelli, S.; Castaldelli, G.; et al. The sacca di Goro lagoon and an arm of the Po river. In *Estuaries*; Springer: Berlin/Heidelberg, Germany, 2006; pp. 197–232. [CrossRef]

26. Maicu, F.; Alessandri, J.; Pinardi, N.; Verri, G.; Umgiesser, G.; Lovo, S.; Turolla, S.; Paccagnella, T.; Valentini, A. Downscaling with an unstructured coastal-ocean model to the Goro Lagoon and the Po River Delta branches. *Front. Mar. Sci.* **2021**, *8*, 647781. [CrossRef]

27. Grilli, F.; Accoroni, S.; Acri, F.; Bernardi Aubry, F.; Bergami, C.; Cabrini, M.; Campanelli, A.; Giani, M.; Guicciardi, S.; Marini, M.; et al. Seasonal and interannual trends of oceanographic parameters over 40 years in the Northern Adriatic Sea in relation to nutrient loadings using the EMODnet Chemistry Data portal. *Water* **2020**, *12*, 2280. [CrossRef]

28. Dalsgaard, T.; Nielsen, L.P.; Brotas, V.; Viaroli, P.; Underwood, G.; Nedwell, D.; Sundback, K.; Rysgaard, S.; Miles, A.; Bartoli, M.; et al. *Protocol Handbook for NICE-Nitrogen Cycling in Estuaries: A Project under the EU Research Programme: Marine Science and Technology (MAST III)*; Ministry of Environment and Energy National Environmental Research Institute, Denmark© Department of Lake and Estuarine Ecology: Silkeborg, Denmark, 2000; pp. 1–62.

29. Owens, M.S.; Cornwell, J.C. The benthic exchange of O_2, N_2 and dissolved nutrients using small core incubations. *JoVE J. Vis. Exp.* **2016**, *114*, e54098. [CrossRef]

30. Nielsen, L.P. Denitrification in sediment determined from nitrogen isotope pairing. *FEMS Microbiol. Lett.* **1992**, *86*, 357–362. [CrossRef]

31. Golterman, H.L.; Clymo, R.S.; Ohnstand, M.A.M. Methods for physical and chemical analysis of fresh waters, I.B.P. In *Handbook Nr. 8*; Blackwell: Oxford, MS, USA, 1978.

32. Bower, C.E.; Holm-Hansen, T. A salicylate–hypochlorite method for determining ammonia in seawater. *Can. J. Fish. Aquat. Sci.* **1980**, *37*, 794–798. [CrossRef]

33. Armstrong, F.A.J.; Stearns, C.R.; Strickland, J.D.H. The measurement of upwelling and subsequent biological process by means of the Technicon Autoanalyzer® and associated equipment. In *Deep Sea Research and Oceanographic Abstracts*; Elsevier: Amsterdam, The Netherlands, 1967; Volume 14, pp. 381–389. [CrossRef]

34. Kana, T.M.; Darkangelo, C.; Hunt, M.D.; Oldham, J.B.; Bennett, G.E.; Cornwell, J.C. Membrane inlet mass spectrometer for rapid high-precision determination of N$_2$, O$_2$, and Ar in environmental water samples. *Anal. Chem.* **1994**, *66*, 4166–4170. [CrossRef]

35. Lunstrum, A.; Aoki, L.R. Oxygen interference with membrane inlet mass spectrometry may overestimate denitrification rates calculated with the isotope pairing technique. *Limnol. Oceanogr. Methods* **2016**, *14*, 425–431. [CrossRef]

36. Eyre, B.D.; Rysgaard, S.; Dalsgaard, T.; Christensen, P.B. Comparison of isotope pairing and N$_2$:Ar methods for measuring sediment denitrification—assumption, modifications, and implications. *Estuaries* **2002**, *25*, 1077–1087. [CrossRef]

37. Weiss, R.F. The solubility of nitrogen, oxygen and argon in water and seawater. In *Deep Sea Research and Oceanographic Abstracts*; Elsevier: Amsterdam, The Netherlands, 1970; Volume 17, pp. 721–735. [CrossRef]

38. Burgin, A.J.; Hamilton, S.K. Have we overemphasized the role of denitrification in aquatic ecosystems? A review of nitrate removal pathways. *Front. Ecol. Environ.* **2007**, *5*, 89–96. [CrossRef]

39. Koop-Jakobsen, K.; Giblin, A.E. Anammox in tidal marsh sediments: The role of salinity, nitrogen loading, and marsh vegetation. *Estuaries Coasts* **2009**, *32*, 238–245. [CrossRef]

40. APAT, IRSA/CNR. Analytical Methods for Water Analysis. 2003. Available online: https://www.isprambiente.gov.it/it/pubblicazioni/manuali-e-linee-guida/metodi-analitici-per-le-acque (accessed on 4 August 2021), ISBN 88-448-0083-7.

41. Hamersley, M.R.; Woebken, D.; Boehrer, B.; Schultze, M.; Lavik, G.; Kuypers, M.M. Water column anammox and denitrification in a temperate permanently stratified lake (Lake Rassnitzer, Germany). *Syst. Appl. Microbiol.* **2009**, *32*, 571–582. [CrossRef]

42. Wallenstein, M.D.; Myrold, D.D.; Firestone, M.; Voytek, M. Environmental controls on denitrifying communities and denitrification rates: Insights from molecular methods. *Ecol. Appl.* **2006**, *16*, 2143–2152. [CrossRef]

43. Dong, L.F.; Sobey, M.N.; Smith, C.J.; Rusmana, I.; Phillips, W.; Stott, A.; Nedwell, D.B. Dissimilatory reduction of nitrate to ammonium, not denitrification or anammox, dominates benthic nitrate reduction in tropical estuaries. *Limnol. Oceanogr.* **2011**, *56*, 279–291. [CrossRef]

44. Asmala, E.; Bowers, D.G.; Autio, R.; Kaartokallio, H.; Thomas, D.N. Qualitative changes of riverine dissolved organic matter at low salinities due to flocculation. *J. Geophys. Res. Biogeosci.* **2014**, *119*, 1919–1933. [CrossRef]

45. Rysgaard, S.; Christensen, P.B.; Nielsen, L.P. Seasonal variation in nitrification and denitrification in estuarine sediment colonized by benthic microalgae and bioturbating infauna. *Mar. Ecol. Prog. Ser.* **1995**, *126*, 111–121. [CrossRef]

46. Christensen, P.B.; Nielsen, L.P.; Sørensen, J.; Revsbech, N.P. Denitrification in nitrate-rich streams: Diurnal and seasonal variation related to benthic oxygen metabolism. *Limnol. Oceanogr.* **1990**, *35*, 640–651. [CrossRef]

47. Seitzinger, S.P. Linkages between organic matter mineralization and denitrification in eight riparian wetlands. *Biogeochemistry* **1994**, *25*, 19–39. [CrossRef]

48. Scott, J.T.; McCarthy, M.J.; Gardner, W.S.; Doyle, R.D. Denitrification, dissimilatory nitrate reduction to ammonium, and nitrogen fixation along a nitrate concentration gradient in a created freshwater wetland. *Biogeochemistry* **2008**, *87*, 99–111. [CrossRef]

49. Nizzoli, D.; Carraro, E.; Nigro, V.; Viaroli, P. Effect of organic enrichment and thermal regime on denitrification and dissimilatory nitrate reduction to ammonium (DNRA) in hypolimnetic sediments of two lowland lakes. *Water Res.* **2010**, *44*, 2715–2724. [CrossRef] [PubMed]

50. Jiang, X.; Gao, G.; Zhang, L.; Tang, X.; Shao, K.; Hu, Y. Denitrification and dissimilatory nitrate reduction to ammonium in freshwater lakes of the Eastern Plain, China: Influences of organic carbon and algal bloom. *Sci. Total Environ.* **2020**, *710*, 136303. [CrossRef] [PubMed]

51. Wang, X.; Hu, M.; Ren, H.; Li, J.; Tong, C.; Musenze, R.S. Seasonal variations of nitrous oxide fluxes and soil denitrification rates in subtropical freshwater and brackish tidal marshes of the Min River estuary. *Sci. Total Environ.* **2018**, *616*, 1404–1413. [CrossRef]

52. Yang, D.; Wang, D.; Chen, S.; Ding, Y.; Gao, Y.; Tian, H.; Chen, Z. Denitrification in urban river sediment and the contribution to total nitrogen reduction. *Ecol. Indic.* **2021**, *120*, 106960. [CrossRef]

53. Sigman, D.M.; Robinson, R.; Knapp, A.N.; Van Geen, A.; McCorkle, D.C.; Brandes, J.A.; Thunell, R.C. Distinguishing between water column and sedimentary denitrification in the Santa Barbara Basin using the stable isotopes of nitrate. *Geochem. Geophys. Geosyst.* **2003**, *4*, 1040. [CrossRef]

54. Dong, L.F.; Thornton, D.C.O.; Nedwell, D.B.; Underwood, G.J.C. Denitrification in sediments of the River Colne estuary, England. *Mar. Ecol. Prog. Ser.* **2000**, *203*, 109–122. [CrossRef]

55. Murphy, A.E.; Bulseco, A.N.; Ackerman, R.; Vineis, J.H.; Bowen, J.L. Sulphide addition favours respiratory ammonification (DNRA) over complete denitrification and alters the active microbial community in salt marsh sediments. *Environ. Microbiol.* **2020**, *22*, 2124–2139. [CrossRef]

56. Trimmer, M.; Nedwell, D.B.; Sivyer, D.B.; Malcolm, S.J. Seasonal benthic organic matter mineralisation measured by oxygen uptake and denitrification along a transect of the inner and outer River Thames estuary, UK. *Mar. Ecol. Prog. Ser.* **2000**, *197*, 103–119. [CrossRef]

57. Seitzinger, S.P. Denitrification in freshwater and coastal marine ecosystems: Ecological and geochemical significance. *Limnol. Oceanogr.* **1988**, *33*, 702–724. [CrossRef]

58. Nowicki, B.L.; Kelly, J.R.; Requintina, E.; Van Keuren, D. Nitrogen losses through sediment denitrification in Boston Harbor and Massachusetts Bay. *Estuaries* **1997**, *20*, 626–639. [CrossRef]

59. Fear, J.M.; Thompson, S.P.; Gallo, T.E.; Paerl, H.W. Denitrification rates measured along a salinity gradient in the eutrophic Neuse River Estuary, North Carolina, USA. *Estuaries* **2005**, *28*, 608–619. [CrossRef]

60. Ogilvie, B.; Nedwell, D.B.; Harrison, R.M.; Robinson, A.; Sage, A. High nitrate, muddy estuaries as nitrogen sinks: The nitrogen budget of the River Colne estuary (United Kingdom). *Mar. Ecol. Prog. Ser.* **1997**, *150*, 217–228. [CrossRef]

61. Nielsen, K.; Nielsen, L.P.; Rasmussen, P. Estuarine nitrogen retention independently estimated by the denitrification rate and mass balance methods: A study of Norsminde Fjord, Denmark. *Mar. Ecol. Prog. Ser.* **1995**, *119*, 275–283. [CrossRef]

62. Whalen, S.C.; Alperin, M.J.; Nie, Y.; Fischer, E.N. Denitrification in the mainstem Neuse River and tributaries, USA. *Fundam. Appl. Limnol.* **2008**, *171*, 249–261. [CrossRef]

63. Bernot, M.J.; Dodds, W.K.; Gardner, W.S.; McCarthy, M.J.; Sobolev, D.; Tank, J.L. Comparing denitrification estimates for a Texas estuary by using acetylene inhibition and membrane inlet mass spectrometry. *Appl. Environ. Microbiol.* **2003**, *69*, 5950–5956. [CrossRef]

64. Li, S.; Twilley, R.R.; Hou, A. Heterotrophic nitrogen fixation in response to nitrate loading and sediment organic matter in an emerging coastal deltaic floodplain within the Mississippi River Delta plain. *Limnol. Oceanogr.* **2021**, *66*, 1961–1978. [CrossRef]